Tunneling Dynamics of interacting bosons in a quantum seesaw potential

IOP Conf. Series: Journal of Physics: Conf. Series **1290** (2019) 012030 doi:10.1088/1742-6596/1290/1/012030

Tunneling Dynamics of interacting bosons in a quantum seesaw potential

Sunayana Dutta[1,*], Budhaditya Chatterjee[2], Pankaj Kumar Mishra[1], Axel U. J. Lode[3,4], Marios C. Tsatsos[5], and Saurabh Basu[1]

[1] Department of Physics, Indian Institute of Technology Guwahati, Assam, India
[2] Department of Physics, Indian Institute of Technology Kanpur, India
[3] Wolfgang Pauli Institute c/o Faculty of Mathematics, University of Vienna, Oskar-Morgenstern Platz 1, 1090 Vienna, Austria
[4] Vienna Center for Quantum Science and Technology, Atominstitut, TU Wien, Stadionallee 2, 1020 Vienna, Austria
[5] São Carlos Institute of Physics, University of São Paulo, P.O. Box 369, 13560-970 São Carlos, São Paulo, Brazil.

E-mail: * sunayanadutta@iitg.ac.in

Abstract. We study the tunneling dynamics of $N = 10$ one-dimensional interacting bosons confined in a temporally driven double well potential that imitates a quantum seesaw and how we can manipulate these dynamics by changing the drive of the seesaw potential. We emulate the seesaw with a driven double well potential and consider two driving protocols: an harmonic constant-frequency drive and a chirped drive with linearly increasing frequency. We consider the time-dependent many-body Schrödinger equation of a repulsively interacting quasi-one-dimensional few-boson system. We solve it by using the multiconfigurational time-dependent Hartree method for bosons (MCTDHB) as implemented in the MCTDH-X software. For an harmonic drive and at small values of the driving amplitude, the dynamics of the particles become very slow rendering a stationary-like state. In a phase-space picture the population imbalance between the wells follows a trajectory which is restricted to a comparatively small region of space. For an harmonic drive at intermediate amplitudes, the dynamics become periodic in nature, implying that the bosons populate each of wells periodically. At comparatively large amplitudes of the harmonic drive, the dynamics show features of chaos in phase-space representation. For the chirped drive with a driving frequency increasing linearly in time, the imbalance of the atoms in the seesaw, however, has a temporal evolution that is faster for certain frequency ranges. The tunneling dynamics in such cases, for small amplitudes, show the appearance of quasi-periodicity with simultaneously present slow and fast oscillations. Increasing the amplitude of the chirped drive, we observe that the dynamics, although being periodic, become severely damped in their amplitude. Our study establishes that by tuning the temporal evolution of the quantum seesaw, a precise control of tunneling dynamics of the correlated bosons can be achieved. Since harmonic driving and chirp frequency modulation of the seesaw are experimentally achievable, our simulations can be experimentally realized in laboratories dealing with cold atomic gases.

1. Introduction

The experimental realization of periodically driven systems such as ultracold atoms in a periodically shaken optical lattice has received significant attention in the quantum physics community. One prototype of these systems is a kicked top or kicked rotor model where

periodic kicks are subjected to a particle moving on a ring [1]. Dynamical Anderson localization [2, 3], dynamical stabilization in the classical or quantum limit, and coherently controlled phase transitions from a superfluid to a Mott insulator [4] represent prominent features of such periodically driven systems.
A significant amount of literature exists in the field of driven Bose-Einstein condensates [5, 6]. In particular, a periodic drive can be used to control the tunneling and interaction parameters and, thereby, provide the possibility to bias the many-body states and quantum phases of Bose-Einstein condensates [7, 8, 9] in the context of optical lattices. Recently, the experimental realization of such systems led to the realization of many-body localization [10, 11] and other exotic physical phenomena.
The efficacious experimental realization of Bose-Einstein condensates in optical lattices has provided a suitable paradigm to study different exotic quantum phenomena of ultracold atoms [12]. Theoretically, the static and dynamic properties of Bose-Einstein condensates are conventionally modeled by the Gross-Pitaevskii mean-field theory (GPE). This theory is an excellent model for explaining non-correlated bosonic systems, albeit with the limitation that it cannot accurately describe correlation effects that may arise dynamically due to the presence of interactions. The usage of only one single-particle state (orbital) to describe a condensate prevents the GPE from explaining correlations which are intrinsically multi-orbital features. We name here the emergence of fragmentation [13, 14, 15, 16, 17, 18, 19, 20, 21, 22, 23, 24, 25, 26, 27, 28, 29, 30, 31] and the superfluid-to-Mott-insulator phase transition [27, 29, 31] as examples. Recently an essentially exact, numerically efficient and multi-orbital many-body theory was developed; the multiconfiguration time-dependent Hartree approach (MCTDH). The bosonic version of MCTDH, the MCTDH for bosons (MCTDHB) [32, 33, 34, 35] represents a systematic generalization of the (one-orbital) Gross-Pitaevskii mean-field theory.
In this work, we use the MCTDHB method to investigate the tunneling dynamics of bosons with contact interactions that are confined in a temporally driven double-well potential with a periodically oscillating spatial bias that imitates a *quantum seesaw*. Our main observable is the imbalance of the number of atoms in the left and the right well as a function of time. We consider two driving protocols: an harmonic, constant-frequency drive and a chirped drive with a frequency linearly increasing in time.
Our paper is structured as follows: In Sec. 2 we discuss the MCTDHB method, in Sec. 3 we discuss the system we study and its physics, and conclude in Sec. 4.

2. MCTDHB method

The dynamics of interacting many-body systems of indistinguishable bosonic particles are described by the time-dependent many-body Schrödinger equation. Usually, this problem is solved by the mean-field approximation [36, 37] or the Bose-Hubbard (BH) model [38, 39]. Here we go beyond these models and employ the fully variational multiconfigurational time-dependent Hartree for bosons (MCTDHB) approach [32, 33, 34, 35]. In the MCTDHB model, which we discuss in the following, there is no restriction on the number of orbitals, geometry, dimensionality, and interparticle interactions of the time-dependent many-boson problem.
The time-evolution of N correlated bosons is governed by the time-dependent many-particle Schrödinger equation (TDSE).
To scale the Hamiltonian and our calculations into dimensionless units, we divide it by $\hbar^2/(2mL^2)$, where m is the mass of the considered boson and L a convenient length scale.
The TDSE reads:

$$\hat{H}\Psi = i\frac{\partial\Psi}{\partial t}. \tag{1}$$

Here, the Hamiltonian $\hat{H}$ is

$$\hat{H}(x_1, x_2, ..., x_N) = \sum_{j=1}^{N} \hat{h}(x_j) + \sum_{k>j=1}^{N} \hat{W}(x_j - x_k), \tag{2}$$

where x_j is the position of the j^{th} boson. The first term of Eq.(2), $\hat{h}$, is the one-body Hamiltonian

$$\hat{h}(x) = \hat{T}(x) + \hat{V}_{trap}(x, t), \tag{3}$$

where $\hat{T}(x)$ is the kinetic energy and $\hat{V}(x,t)$ is the external potential or the trapping potential. The second term in Eq. (2), $\hat{W}(x_j - x_k) = \lambda_0 \delta(x_j - x_k)$ is the two-body interaction of the bosonic gas. In this work, as is conventional for Bose-Einstein condensates [37], $\hat{W}$ is approximated as a contact interaction.
Here λ_0 is the interaction strength and is scaled with the total number of particles as, $\lambda_0 = \lambda/(N-1)$.
The use of time-adaptive optimized basis states is the key idea of the MCTDHB approach. In second quantization, the bosonic field operator corresponding to a set of M orthonormal, time-dependent functions (orbitals) $\{\phi_k(x,t)\}$ which annihilates a particle at position x can be written as,

$$\hat{\Psi}(x,t) = \sum_{k=1}^{M} \hat{a}_k \phi_k(x,t). \tag{4}$$

The bosonic creation and annihilation operators obey the usual commutation relations at any instant t. With the help of the bosonic creation operators, $\hat{a}_k^\dagger$, time-dependent permanents can be expressed as

$$|\vec{n}; t\rangle = \frac{[a_1^\dagger(t)]^{n_1}[a_2^\dagger(t)]^{n_2}...[a_M^\dagger(t)]^{n_M}}{\sqrt{n_1! n_2! n_3! ... n_M!}}|0\rangle \tag{5}$$

where $\vec{n} = (n_1, n_2, n_3, ...n_M)$ are the occupations of the orbitals which conserve the total number of particles as $n_1 + n_2 + ... + n_M = N$. These time-dependent permanents are used as the basis set in MCTDHB.
The ansatz made for the many-boson wave function in MCTDHB is:

$$|\Psi(t)\rangle = \sum_{n} C_{\vec{n}}(t)|\vec{n}; t\rangle. \tag{6}$$

The summation in Eq. (6) runs over all possible configurations, that can be obtained by distributing N bosons in M orbitals. In the limit $N \to \infty$ the permanents $|\vec{n}; t\rangle$ span the N-bosons Hilbert space and the variational principle [40] guarantees that the solutions of the time-dependent many-body problem provided by the MCTDHB method are exact [41, 35].
To derive the MCTDHB equations we use the time-dependent variational principle (TDVP) [40] to determine the time evolution of the expansion coefficients $\{C_{\vec{n}}(t)\}$ and the orbitals $\{\phi_k(\mathbf{r}, t)\}$ [33, 34].
In the following picture the MCTDHB equations are obtained by fixing the gauge freedom in the choice of the orbitals by the condition $\langle \frac{\partial \phi_j}{\partial t} | \phi_k \rangle = 0, \forall j, k \in [1, M]$.
The variation of the action with respect to the expansion coefficients $C_{\vec{n}}(t)$ yields the equations of motion for the expansion coefficients [33, 34],

$$\sum_{\vec{n}} \mathcal{H}_{\vec{n}\vec{n}'}(t) C_{\vec{n}} = i \frac{\partial C_{\vec{n}'(t)}}{\partial t} \tag{7}$$

This equation of motion is a first-order differential equation and the matrix $\mathcal{H}_{\vec{n}\vec{n}'}(t) = \langle\vec{n};t|\hat{H}|\vec{n}';t\rangle$ is time-dependent as the permanents $|\vec{n};t\rangle$ and $\hat{H}$ itself are functions of time.
The variation of the action with respect to the orbitals $\{\phi_k(x,t)\}$ yields the equation of motion for the orbitals [33, 34]:

$$i|\dot{\phi_j}\rangle = \hat{\mathbf{P}}[\hat{h}|\phi_j\rangle + \sum_{k,s,q,l=1}^{M} \{\rho(t)\}^{-1}_{jk}\rho_{ksql}\hat{W}_{sl}|\phi_q\rangle] \tag{8}$$

where

$$\hat{\mathbf{P}} = 1 - \sum_{j=1}^{M} |\phi_j\rangle\langle\phi_j| \tag{9}$$

$\rho_{jk} = \langle\Psi|\hat{a}^\dagger_j\hat{a}_k|\Psi\rangle$ are the matrix elements of the one-body reduced density matrix (RDM) and $\rho_{ksql} = \langle\Psi|\hat{a}^\dagger_k\hat{a}^\dagger_s\hat{a}_l\hat{a}_q|\Psi\rangle$ are the matrix elements of the two-body RDM. The local interaction potentials read $\hat{W}_{sl} = \int dx'\phi^*_s(x',t)W(x,x')\phi_l(x',t)$. For the contact interactions that we consider in this paper, the $\hat{W}_{sl}$ are given by $\hat{W}_{sl} = \lambda_0\phi^*_s(x,t)\phi_l(x,t)$.

3. Results

In this work, we consider $N = 10$ bosons in one spatial dimension interacting via contact interaction trapped in a driven double well potential $V_{trap}(x,t)$ that imitates a quantum seesaw:

$$V_{trap}(x,t) = V_0\cos^2(x) - \alpha x[\cos(\omega t) + \cos(\beta t^2)]. \tag{10}$$

Here V_0 is the barrier height of the trapping potential and αx is the relative tilt between the two wells. The parameter α thus corresponds to the strength of the drive of our quantum seesaw. By tuning the frequency ω, we drive the tilt of the seesaw harmonically and by tuning the parameter β we drive the tilt of the seesaw with a chirp, i.e. a frequency βt that linearly increases in time. In our analysis below, we choose the interaction strength of the bosons $\lambda_0 = 0.05$, the barrier height $V_0 = 10$, and the strength of the driving force α between 0 to 8. Our numerical grid extends from $x_{min} = -\pi$ to $x_{max} = +\pi$.
We simulate the dynamics with the MCTDH-X software package [42, 43, 44] using $M = 3$ orbitals for all calculations.
As the initial state for our computations, we use the ground state of the interacting bosons in the potential $V_{trap}(x,t)$ with $\alpha \equiv 0$ in Eq. (10).
Fig. 1 shows snapshots of the temporally oscillating double well potential at various instants of time.
To get an intuitive idea about the dynamical behavior of the system in the driven seesaw-potential, we systematically investigate the time-evolution of the population imbalance between the wells,

$$n(t) = N - \int_0^\infty \rho(x,t)dx. \tag{11}$$

Here, N is the number of bosons and $\rho(x) = \langle\Psi|\hat{\Psi}^\dagger(x,t)\hat{\Psi}(x,t)|\Psi\rangle$ is the one-body density.
We visualize the imbalance $n(t)$ by plotting it as a function of time and by analyzing it in a "phase-space representation". To obtain this phase-space representation, we plot points $[n(t), n(t+\tau)]$ as a function of time t for a fixed τ. From these phase-space plots, we are able to distinguish different kinds of dynamics as function the driving protocol [α, ω, β in Eq. (10)] of our quantum seesaw.

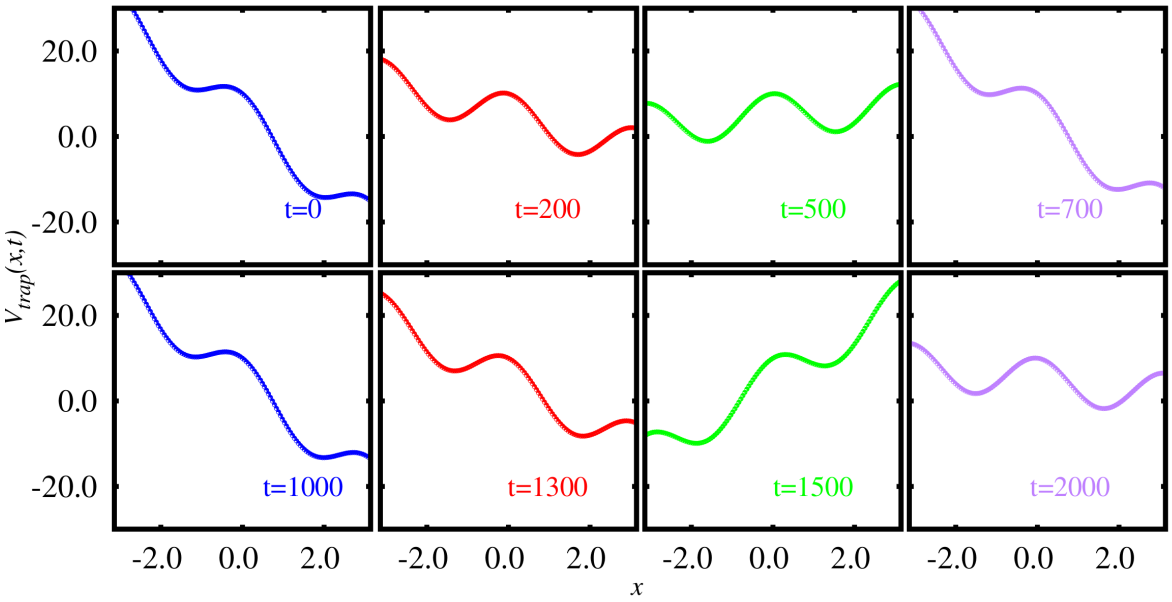

Figure 1. (Color online) Quantum seesaw potential as a function of time. This figure shows snapshots of the temporally driven double well in Eq. (10) potential for several times t for a chirped driven ($\omega = 0, \beta = 1, V_0 = 10$) tilt of amplitude $\alpha = 8$.

In the following, we exhibit our main result, the physics of the time-evolution of the population imbalance as a function of the force α that drives the seesaw. We showcase two different driving protocols for the seesaw, a harmonic drive ($\omega \neq 0$ and $\beta = 0$) and chirped drive ($\omega = 0$ and $\beta \neq 0$) in Subsections 3.1 and 3.2, respectively.

3.1. Harmonic driving ($\omega \neq 0$ and $\beta = 0$)

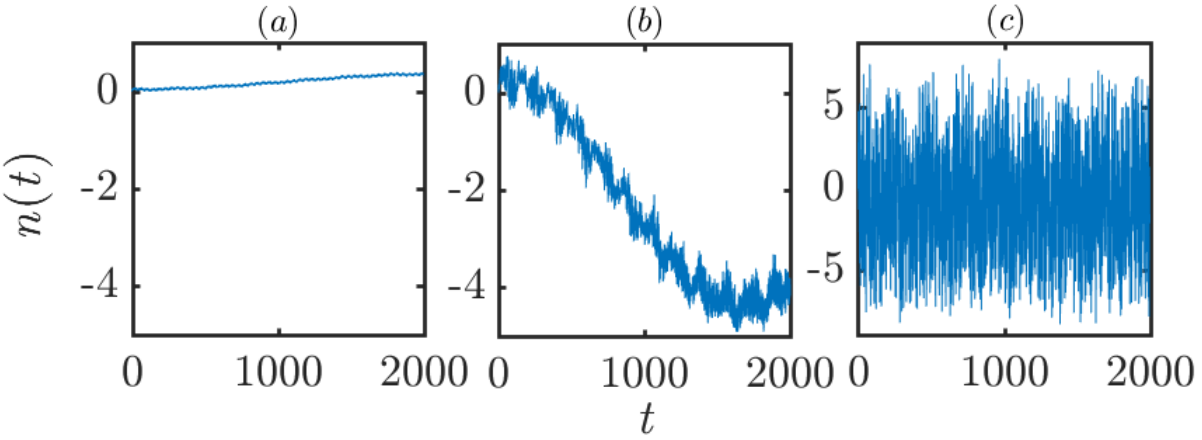

Figure 2. (Color online) Time-evolution of the population imbalance $n(t)$ for the harmonic drive ($\omega = 1$ and $\beta = 0$), for driving amplitudes $\alpha = 1$ (a), $\alpha = 3$ (b), and $\alpha = 8$ (c). See text for further discussion.

We drive our seesaw harmonically, i.e., with a constant frequency by choosing $\omega = 1$ and $\beta = 0$ in the trapping potential Eq. (10). At a small value of the driving amplitude of the seesaw,

$\alpha = 1$, we observe that the dynamics of the population imbalance of the bosons, $n(t)$, happen on a very long time-scale [Fig. 2(a)]. For larger amplitude driving, $\alpha = 3$, we find a periodic time-evolution of the imbalance $n(t)$ with a large period [see Fig. 2(b)]. For drives with very large amplitudes, $\alpha = 8$, the dynamics of the imbalance $n(t)$ start to feature fast oscillations [Fig. 2(c)]; the oscillations are much faster than those for intermediate and small amplitude drives depicted in [Fig. 2(a) and (b), respectively].

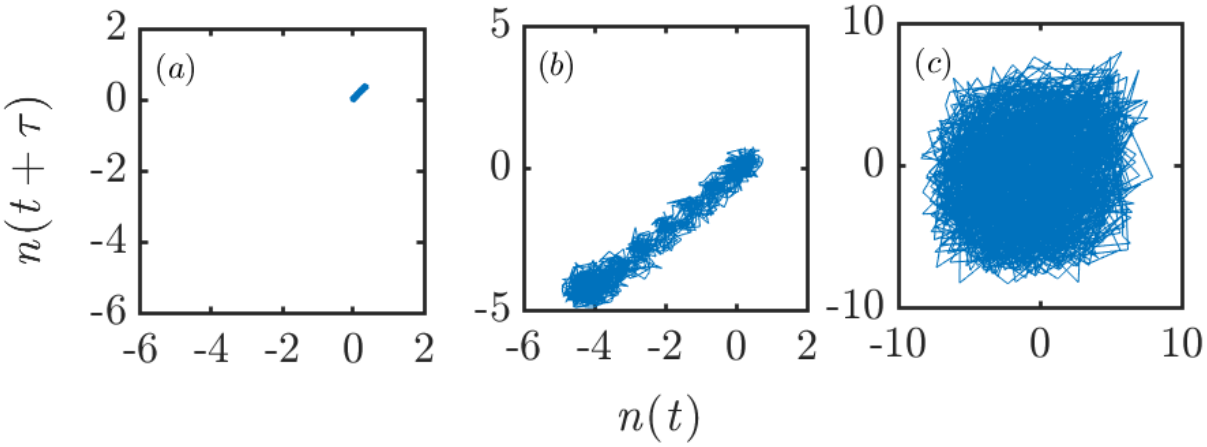

Figure 3. (Color online) Phase-space depiction of the time-evolution of the population imbalance $[n(t), n(t+\tau)]$ for the harmonic drive ($\omega = 1$ and $\beta = 0$), for driving amplitudes $\alpha = 1$ (a), $\alpha = 3$ (b), and $\alpha = 8$ (c). All panels show points $[n(t), n(t+\tau)]$ as a function of the time t for fixed $\tau = 50$. See text for further discussion.

We now analyze the phase-space representation of the population imbalance. We plot points $[n(t), n(t+\tau)]$ as a function of the time t for a fixed $\tau = 50$ in Fig. 3. For a small driving amplitude, $\alpha = 1$, the system behaves almost like a stationary state and very little of the available phase space is explored [Fig. 3(a)]. As the drive amplitude increases ($\alpha = 3, 8$), the trajectory of $[n(t), n(t+\tau)]$ explores increasing portions of the available phase space, Fig. 3(b) and (c). The $[n(t), n(t+\tau)]$ trajectory for the largest drive amplitude $\alpha = 8$ in Fig. 3(c) bears resemblance to trajectories expected for chaotic systems as it emphasizes that a large region of the phase space is visited multiple times by the system.

3.2. Chirping modulation ($\omega = 0$ and $\beta \neq 0$)

Now we consider a chirped drive of our quantum seesaw [$\omega = 0$ and $\beta = 1$ in Eq.(10)]. For small driving amplitudes ($\alpha = 1$), the tunneling dynamics in the chirped seesaw result in a quasi-periodic population imbalance: $n(t)$ shows oscillations that feature two frequencies – a small and a large one – see Fig. 4(a). When the amplitude of the drive is increased ($\alpha = 8$), the dynamics of $n(t)$ stay periodic with two frequencies; however, the amplitude of the oscillations in $n(t)$ is damped and the frequencies are changed in comparison to small driving amplitudes [compare Fig. 4(a) and (b)].

We now turn to the phase-space representation of the time-evolution of the population imbalance and plot $[n(t), n(t+\tau)]$ as a function of time t for $\tau = 50$ in Fig. 5. For small driving amplitudes [$\alpha = 1$, Fig. 5(a)] the phase-space representation shows an elliptical trajectory depicting the Rabi oscillations at a small frequency. The additional "curls" on this elliptical curve are the consequence of the second, larger, observed frequency in the oscillations of the imbalance [compare Fig. 4(a) and Fig. 5(a)]. For larger-amplitude chirped drives ($\alpha = 8$), we find a phase-space trajectory that is confined within a small volume of the available phase space, see

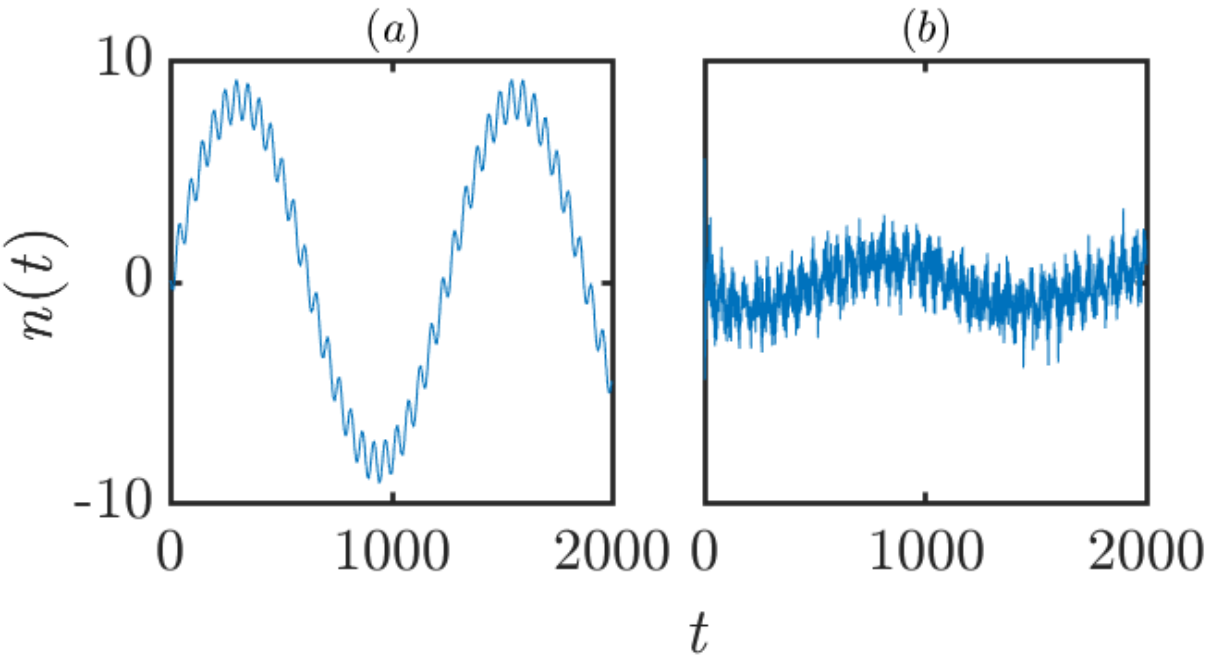

Figure 4. (Color online) Time-evolution of the population imbalance $n(t)$ for the chirped drive ($\omega = 0$ and $\beta = 1$), for driving amplitudes $\alpha = 1$ (a) and $\alpha = 8$ (b). See text for further discussion.

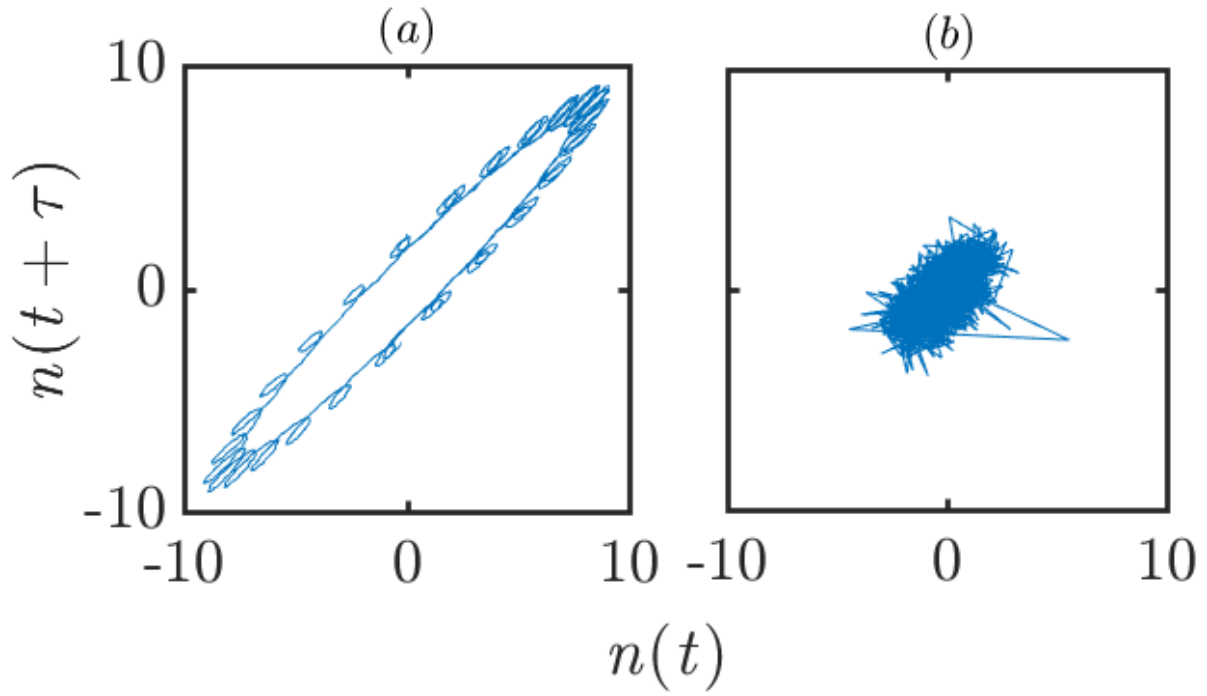

Figure 5. (Color online) Phase-space depiction of the time-evolution of the population imbalance $[n(t), n(t+\tau)]$ for the chirped drive of the seesaw ($\omega = 0$ and $\beta = 1$), for driving amplitudes $\alpha = 1$ (a) and $\alpha = 8$ (b). All panels show points $[n(t), n(t+\tau)]$ as a function of the time t for fixed $\tau = 50$. See text for further discussion.

Fig. 5(b). The observation of this confinement to a small volume of the available phase space is in mutual agreement with the smaller-amplitude oscillations of the imbalance [compare Fig. 4(b) and Fig. 5(b)].

4. Conclusions

We have investigated the tunneling dynamics of the quantum seesaw, a system of interacting bosons trapped in a temporally driven double-well potential.

We studied a harmonic drive of the seesaw with a constant frequency and a chirped drive of the seesaw with a frequency that increases linearly in time.

For the harmonic drive, at small values of the driving amplitude, the dynamics of the almost stationary system are very slow. The phase-space trajectory of the system is restricted to very limited region of the available phase space. For intermediate amplitudes of the drive, the dynamics become periodic in nature; the bosons populate different wells periodically in time. For large-amplitude drives, the periodicity disappears, the imbalance features fast oscillations, and – in phase-space representation – the dynamics resemble those of chaotic systems.

For a chirped drive of the quantum seesaw, we find quasi-periodic tunneling dynamics of the system: the time-evolution of the population imbalance features a small and a large frequency modulation with large and small amplitude, respectively. For chirped drives with a large amplitude, we observe similar two-frequency dynamics of the imbalance, but at a severely impeded amplitude with different frequencies as for small-amplitude chirped drives.

Our study thus establishes that by tuning the temporal evolution of the quantum seesaw, a precise control of tunneling dynamics of correlated bosons can be achieved. Since harmonic driving and chirped frequency modulation of the seesaw are experimentally achievable, our simulations can be experimentally realized in laboratories dealing with cold atomic gases.

As an outlook, it would be interesting to study the effects we found as a function of the interaction strength of the system. Furthermore, it would be highly interesting to understand how the observed different dynamical behaviors in the quantum seesaw are complemented by the many-body properties like the Glauber correlation functions [45] or the fragmentation [13, 14, 15, 16, 17, 18, 19, 20, 21, 22, 23, 24, 25, 26, 27, 28, 29, 30, 31] of the system.

References

[1] *Stochastic Behavior of a Quantum Pendulum under a Periodic Perturbation, in Stochastic Behavior in Classical and Quantum Hamiltonian Systems*, Lecture Notes in Physics, Vol. 93, G. Casati, B. V. Chirikov, F. M. Izraelev, and J. Ford, edited by Giulio Casati and Joseph Ford, Berlin Heidelberg; Springer (1979).
[2] F. Haake, M. Kus, and R. Scharf, Z. Phys. B **65**, 381 (1986); *Quantum Signatures of Chaos*, F. Haake, Berlin; Springer (2001); S. Fishman, D. R. Grempel, and R.E. Prange, Phys. Rev. Lett. **49**, 509 (1982).
[3] *The Transition to Chaos: Conservative Classical Systems and Quantum Manifestations*, L. E. Reichl, New York; Springer (2004).
[4] A. Eckardt, C. Weiss, and M. Holthaus, Phys. Rev. Lett. **95**, 260404 (2005).
[5] S. Longhi, J. Phys. B: At. Mol. Opt. Phys. **44**, 051001 (2011).
[6] K. Winkler, G. Thalhammer, F. Lang, R. Grimm, J. Hecker Denschlag, A. J. Daley, A. Kantian, H. P. Büchler, and P. Zoller, Nature **441**, 853 (2006).
[7] H. L. Haroutyunyan and G. Nienhuis, Phys. Rev. A **70**, 063603 (2004); G. Watanabe and H. Mäkelä, Phys. Rev. A **85**, 053624 (2012); W. Hai, C. Lee, G. Chong, and L. Shi, Phys. Rev. E **66**, 026202 (2002); G. L. Salmond, C. A. Holmes, and G. J. Milburn, Phys. Rev. A **65**, 033623 (2002).
[8] X. Luo, Q. Xie, and B. Wu, Phys. Rev. A **77**, 053601 (2008).
[9] J. Gong, L. Morales-Molina, and P. Hänggi, Phys. Rev. Lett. **103**, 133002 (2009).
[10] P. Ponte, Z. Papi, F. Huveneers, and D. A. Abanin, Phys. Rev. Lett. **114**, 140401 (2015); P. Bordia, H. Lschen, U. Schneider, M. Knap, and I. Bloch, Nature Physics **13**, 460 (2017).
[11] A. Eckardt, M. Holthaus, H. Lignier, A. Zenesini, D. Ciampini, O. Morsch, and E. Arimondo, Phys. Rev. A **79**, 013611 (2009).
[12] M. H. Anderson, J. R. Ensher, M. R. Matthews, C. E. Wiemann, and E. A. Cornell, Science **269**, 198 (1995).

[13] A. U. J. Lode, A. I. Streltsov, K. Sakmann, O. E. Alon, and L. S. Cederbaum *How does an interacting many-body system tunnel through a potential barrier to open space?*, Proc. Natl. Acad. Sci. USA **109**, 13521 (2012).
[14] I. Brezinova, A. U. J. Lode, A. I. Streltsov, O. E. Alon, L. S. Cederbaum, and J. Burgdörfer, *Wave chaos as signature for depletion of a Bose-Einstein condensate* Phys. Rev. A **86**, 013630 (2012).
[15] J. Grond, A. I. Streltsov, A. U. J. Lode, K. Sakmann, L. S. Cederbaum, and O. E. Alon, *Excitation spectra of many-body systems by linear response: General theory and applications to trapped condensates*, Phys. Rev. A **88**, 023606 (2013).
[16] I. Brezinova, A. U. J. Lode, A. I. Streltsov, L. S. Cederbaum, O. E. Alon, L. A. Collins, B. I. Schneider, and J. Burgdörfer *Elastic scattering of a Bose-Einstein condensate at a potential landscape*, J. Phys.: Conf. Ser. **488**, 012032 (2014).
[17] S. Klaiman, A. U. J. Lode, A. I. Streltsov, L. S. Cederbaum, and O. E. Alon, *Breaking the resilience of a two-dimensional Bose-Einstein condensate to fragmentation*, Phys. Rev. A **90**, 043620 (2014).
[18] M. C. Tsatsos and A. U. J. Lode, *Vortex nucleation through fragmentation in a stirred resonant Bose-Einstein condensate*, J. L. Temp. Phys. **181**, 171 (2015).
[19] A. U. J. Lode, B. Chakrabarti, and V. K. B. Kota, *Many-body entropies, correlations, and emergence of statistical relaxation in interaction quench dynamics of ultracold bosons*, Phys. Rev. A **92**, 033622 (2015).
[20] U. R. Fischer, A. U. J. Lode, and B. Chatterjee, *Condensate fragmentation as a sensitive measure of the quantum many-body behavior of bosons with long-range interactions*, Phys. Rev. A **91**, 063621 (2015).
[21] A. U. J. Lode and C. Bruder, *Dynamics of Hubbard Hamiltonians with the multiconfigurational time-dependent Hartree method for indistinguishable particles*, Phys. Rev. A **94**, 013616 (2016).
[22] S. E. Weiner, M. C. Tsatsos, L. S. Cederbaum, and A. U. J. Lode, *Phantom vortices: hidden angular momentum in ultracold dilute Bose-Einstein condensates*, Scientific Reports **7**, 40122 (2017).
[23] A. U. J. Lode and C. Bruder, *Fragmented Superradiance of a Bose-Einstein Condensate in an Optical Cavity*, Phys. Rev. Lett. **118**, 013603 (2017).
[24] M. C. Tsatsos, J. H. V. Nguyen, A. U. J. Lode, G. D. Telles, D. Luo, V. S. Bagnato, and R. G. Hulet, *Granulation in an atomic Bose-Einstein condensate*, arXiv:1707.04055 (2017).
[25] B. Chatterjee and A. U. J. Lode, *Order parameter and detection for crystallized dipolar bosons in lattices*, arXiv:1708.07409 (2017).
[26] P. Molignini, L. Papariello, A. U. J. Lode, R. Chitra, *Superlattice switching from parametric instabilities in a driven-dissipative BEC in a cavity*, arXiv:1710.02474 (2017).
[27] R. Roy, A. Gammal, M. C. Tsatsos, B. Chatterjee, B. Chakrabarti, and A. U. J. Lode, *Phases, many-body entropy measures and coherence of interacting bosons in optical lattices*, Phys. Rev. A **97**, 043625 (2018).
[28] A. U. J. Lode, F. S. Diorico, R. Wu, P. Molignini, L. Papariello, R. Lin, C. Lévêque, L. Exl, M. C. Tsatsos, R. Chitra, and N. J. Mauser, *Many-body physics in two-component Bose-Einstein condensates in a cavity: fragmented superradiance and polarization*, New J. Phys. **20**, 055006 (2018).
[29] S. Dutta, M. C. Tsatsos, S. Basu, and A. U. J. Lode, *Management of the Correlations of Ultracold Bosons in Triple Wells*, arXiv:1802.02407 (2018).
[30] S. Bera, B. Chakrabarti, A. Gammal, M. C. Tsatsos, M. L. Lekala, B. Chatterjee, C. Lévêque, and A. U. J. Lode, *Sorting Fermionization from Crystallization in Many-Boson Wavefunctions*, arXiv:1806.02539 (2018).
[31] B. Chatterjee, M. C. Tsatsos, and A. U. J. Lode, *Correlations of strongly interacting ultracold dipolar bosons in optical lattices*, arXiv:1806.05048 (2018).
[32] A. I. Streltsov, O. E. Alon, and L. S. Cederbaum, Phys. Rev. Lett. **99**, 030402 (2007).
[33] O. E. Alon, A. I. Streltsov, and L. S. Cederbaum, Phys. Rev. A **77**, 033613 (2008).
[34] K. Sakmann, *Many-body Schrödinger dynamics of Bose-Einstein condensates*, Springer Theses, (Springer, 2011).
[35] A. U. J. Lode, *Tunneling Dynamics in Open Ultracold Bosonic Systems*, Springer Theses, (Springer, Heidelberg, 2014).
[36] *Bose-Einstein Condensation in Dilute Gases*, C. J. Pethick and H. Smith, (Cambridge University Press, Cambridge UK, 2002).
[37] *Bose-Einstein Condensation*, L.P. Pitaevskii and S. Stringari, (Clarendon Press, Oxford, 2003).
[38] M. Greiner, O. Mandel, T. Esslinger, T. W. Hänsch, and I. Bloch, Nature **415**, 39 (2002).
[39] D. Jaksch, C. Bruder, J. I. Cirac, C. W. Gardiner, and P. Zoller, Phys. Rev. Lett. **81**, 3108 (1998).
[40] *Geometry of the time-dependent variational principle*, P. Kramer and M. Saracen, (Springer, Berlin, 1981).
[41] A. U. J. Lode, K. Sakmann, O. E. Alon, L. S. Cederbaum, and A. I. Streltsov, *Exact quantum dynamics of bosons with finite-range time-dependent interactions of harmonic type*, Phys. Rev. A **86**, 063606 (2012).
[42] A. U. J. Lode, Phys. Rev. A **93**, 063601 (2016).
[43] E. Fasshauer and A. U. J. Lode, Phys. Rev. A **93**, 033635 (2016).
[44] A. U. J. Lode, M. C. Tsatsos, E. Fasshauer, R. Lin, L. Papariello, P. Molignini, and C. Lévêque,

MCTDH-X: *The time-dependent multiconfigurational Hartree for indistinguishable particles software*, http://ultracold.org (2018).
[45] R. J. Glauber, Phys. Rev. **130**, 2529 (1963).